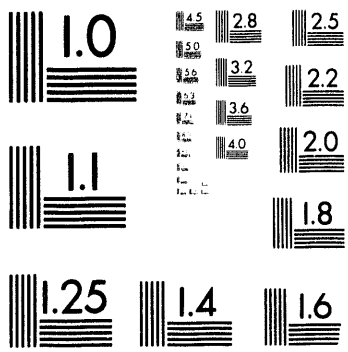
1.0
1.1
1.25
1.4
1.6
1.8
2.0
2.2
2.5
2.8
3.2
3.6
4.0
4.5
5.0
5.6

1 of 1

Simulation of Penetration and Perforation with CTH

S. A. Silling

Computational Physics and Mechanics Department, 1432
Sandia National Laboratories
Albuquerque, New Mexico 87185

ABSTRACT

Recent developments in the specialization and application of the CTH code to penetration and perforation problems are reviewed. The three-dimensional version of the boundary layer algorithm, which enhances the accuracy of Eulerian simulations involving sliding contact between solids, is described and demonstrated.

1.0 Introduction

CTH (McGlaun, Thompson, and Elrick, 1990) is an Eulerian code for the simulation of dynamic problems involving large stresses and deformations. *Eulerian* means that the mesh is fixed in space, and material is advected between the numerical cells. This is in contrast to *Lagrangian* codes, in which each numerical node is attached to a material particle, so the mesh moves along with the material.

The Eulerian approach has certain advantages for simulating problems involving penetration or perforation. Such problems invariably involve very large deformation, particularly in the vicinity of the tip of the penetrator. Eulerian codes have the inherent advantage of being able to handle arbitrarily large deformation without suffering the ill effects due to mesh distortion which characterize Lagrangian simulations of these types of problems. However, Eulerian approaches also have disadvantages as well. One is that they tend to require finer meshes in order to achieve adequate spatial resolution for typical problems. The greatest difficulty in applying Eulerian codes to penetration and perforation problems has been the difficulty in treating sliding interfaces between solids. The origin of this difficulty is that it is impossible to resolve the details of interactions between solid materials within a mixed cell containing the material interface. This effect can lead to incorrect predictions of changes in shape of a penetrator surface. For a graphic example of this inappropriate distortion, see Silling (1992a).

A new algorithm has been developed and installed in CTH for the improved treatment of sliding interfaces (Silling, 1992b). This method, called the *boundary layer algorithm,* avoids the problem of excessive numerical erosion. It also allows for friction across a sliding interface. The two-dimensional version is now available in the production version of CTH, and development of the three-dimensional version is nearly complete. This algorithm greatly enhances the accuracy of CTH in modeling penetration and perforation, particularly when the impact velocity is too low for erosion of the penetrator to be significant. The purpose of this paper is to review the status and capabilities of CTH, using this algorithm, in modeling penetration and perforation.

2.0 Numerical Methods

2.1 Lagrangian and Remap Steps

In CTH, the numerical solution scheme proceeds by first moving the mesh through displacements determined by the material velocity field, and then remapping the mesh back to its original position. These two steps are called the *Lagrangian* and *remap* steps respectively, and they are both performed at each time increment.

The formulation of the Lagrangian step is identical to that found in typical Lagrangian finite difference wavecodes (Herrmann and Bertholf, 1983). Since the mesh is always rectangular at the start of each time increment (because of the remap step in the previous time increment), the difference equations are quite simple. The stress tensor components and mass densities are cell centered quantities, while the velocity vector components are centered at the cell faces. Following the Lagrangian step, all of the velocities at the cell faces are known.

This is followed by the remap step, which convects mass and energy for each material between neighboring cells. Other quantities, such as internal state variables used in constitutive models for certain material, are also convected. The algorithm used for the convection is a second-order accurate method developed by Van Leer (1977). This method provides greater accuracy than earlier, first-order accurate methods.

Constitutive laws are applied at the cell centers following the remap step. For historical reasons, the equation of state (which provides pressure and temperature as a function of mass density and internal energy density) is applied separately from the strength model (which provides the deviatoric stress rate tensor components as functions of the appropriate strain rate tensor variables). The current mass density and internal energy density are obtained for each cell from the total mass, total internal energy, and total volume of each material in each cell. A variety of equations of state is available in CTH, together with parameters for commonly used materials in automated tabular form (Kerley, 1991).

The strength model, at present, is basically confined to isotropic elastic-plastic materials using J_2 flow theory. Options are available for isotropic hardening, thermal softening, and strain-rate dependence of flow stress using the models of Johnson and Cook (1983), Zerilli and Armstrong (1987), and Steinberg and coworkers (Steinberg, Cochran, and Guinan, 1980; Steinberg and Lund, 1989). An option for Mohr-Coulomb yield behavior is available. The model for ceramic materials of Johnson, Holmquist, Lankford, Anderson, and Walker (1990) has also been implemented. Rigid rotations are accounted for using the Jaumann stress rate. The flow rule is implemented using the radial return method (Wilkins, 1969). The code is currently being upgraded to allow, optionally, kinematic hardening, anisotropic behavior, and use of the Green-Naghdi stress rate in the flow rule.

CTH can model material failure due to a critical tensile mean stress (spall) or critical tensile principal stress. A scalar damage model based on shear strain which takes into account triaxiality along the loading path is also available (Johnson and Cook, 1985).

Unlike the equation of state, the strength model in CTH does not allow for different stresses among different materials in a cell. The entire cell is homogenized for purposes of computing the current flow stress, and a single deviatoric stress tensor is applied to the entire cell. Also, a single strain rate tensor is applied to all materials present in a cell. (CTH is a *homogeneous flow* code, meaning that a single set of kinematic variables describes all materials in the mesh.)

As mentioned in the Introduction, this treatment of mixed cells in the strength model leads to trouble in the simulation of penetration and perforation problems. The reason is that material properties tend to become diluted in mixed cells, leading to excessive erosion of a hard material, such as a rigid penetrator, sliding along an interface with a softer material, such as a typical target. A new algorithm,

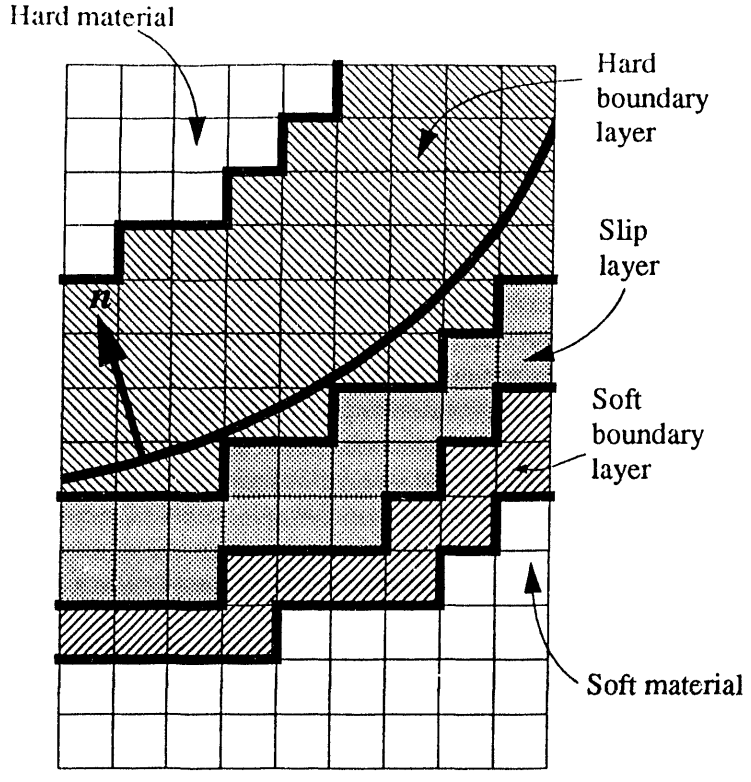

Figure 2.1. Hard and soft boundary layers and slip layer surrounding a material interface.

known as the *boundary layer algorithm,* has been developed to overcome these difficulties. This method will now be summarized.

2.2 Boundary Layer Algorithm

This approach to improving Eulerian simulations of penetration and perforation has been described in detail by Silling (1992a, 1992b). It will be summarized briefly here.

The basic idea is that the process of sliding is moved out of the mixed cells, where it causes the numerical problems referred to above, and into single-material cells containing the softer of the two materials. The method is illustrated in Figure 2.1. The cells near the material interface are designated as belonging to the *hard boundary layer* or the *soft boundary layer* depending on their material content. Within the soft boundary layer lies the *slip layer,* within which cells have their strength, i.e., their deviatoric stress tensors, set to zero. The slip layer is comprised only of cells containing just the softer material. Because the slip layer has zero strength, the process of sliding occurs there rather than in the mixed cells. This simulates a frictionless sliding boundary.

Friction is included by applying body force density fields within the hard and soft boundary layers. The traction due to friction across the material interface is obtained from the normal traction, based on the local stress tensors and the orientation of the surface. The shear traction due to Coulomb friction is then found from this normal traction vector and the friction coefficient. The direction of the friction traction vector is found from the relative velocities of the two materials averaged within a given distance of the cell being computed and the orientation of the interface. This shear traction vector due to friction is converted to a body force density field by dividing it by the local boundary layer thickness.

The reason for applying the friction force as a body force density field is that the obvious alternative, which is to apply it directly to cells along the interface, would require applying forces in opposite

directions to different materials in the same mixed cell. This could not work, because, as mentioned above, there is only one set of kinematic variables, including velocities, for all materials. Therefore, the applied forces within the same cell would simply cancel each other out.

The boundary layer algorithm in two dimensions in CTH has been applied to a variety of problems in penetration and perforation, as well as other applications. The two-dimensional version is currently available for general use. Development of the three-dimensional version is nearly complete.

The numerical methods used in the three-dimensional versions of the boundary layer algorithm are the obvious generalizations of those in the two-dimension method. However, there are programming aspects of the implementation that make the three-dimensional version much more complex. The difficulty lies in the unavailability of data for the complete mesh in central memory. In evaluating the local average stress tensors in the two materials near an interface for purposes of the friction calculation for cell i,j,k, the method requires the stress components in cells some distance away from that cell. Typically, the average stresses among cells in a 9x9x9 block centered at i,j,k are required. However, at any given time in a CTH calculation, only a total of 5 k-planes is present in central memory at once. The data for the remainder of the mesh are in mass storage and cannot be accessed directly. This unavailability greatly complicates the implementation of the method in three dimensions. The issue does not arise in two dimensions, because the entire mesh is always present in central memory.

To overcome this problem, data needed for evaluation of the average values in the boundary layer algorithm are stored on two direct-access scratch files. The direct access files to some extent approximate central memory, since any record may be read or written independently of the others. However, file access is of course slower than access of central memory. In spite of this, the implementation of the three-dimensional algorithm has been refined to the point that in typical problems it increases the execution time by no more than 8%. A very large increase in capability is obtained for this cost, as the examples in the next section show.

The main source of error associated with the boundary layer algorithm is that it causes an effective enlargement of the radius of a penetrator by approximately one half the thickness of the slip layer. This occurs because, by design, the sliding interface is pushed outward from the actual material interface. The result of this error typically is that the penetrator experiences too large a reaction force from the target, because it creates a tunnel that is wider than it should be. However, in many deep penetration problems, this error may be compensated for by increasing the mass of the penetrator by a factor equal to

$$\left(\frac{r_0 + \frac{w_{sl}}{2}}{r_0} \right)^2 , \qquad \text{(EQ 1)}$$

where r_0 is the radius of the penetrator and w_{sl} is the slip layer thickness (an input parameter). This correction is supplied as a user option.

The Eulerian approach with the boundary layer algorithm is simpler than the Lagrangian slideline algorithms which have been under development for many years. The reason is that to model a frictionless sliding interface, the Eulerian approach basically just manipulates the material properties in the slip layer. It does not need to figure out which node is in contact with which element on the opposite side of the slideline; nor does it need to resolve the force vectors between nodes or elements on opposite sides. This simplification eliminates the need for the sophisticated search and force resolution algorithms that play a large part in modern slideline algorithms in three-dimensional Lagrangian codes.

However, Lagrangian codes continue to have some advantages over CTH. In particular, greater spatial resolution is typically required in an Eulerian mesh for a given penetration problem, leading to higher cost. Also, Lagrangian finite element codes are more suitable for analysis of the structural response of a penetrator, as opposed to merely predicting the trajectory, penetration depth, and forces on the body. For these reasons, an effort is currently underway to couple the EPIC Lagrangian finite element code (Johnson and Stryk, 1990) with CTH. The objective is to model the projectile with an EPIC mesh and to model the target material with a CTH mesh. It is hoped that this coupled approach will exploit the advantages of each code and reduce their individual weaknesses.

3.0 Sample Calculations

We now turn to examples of CTH calculations of penetration and perforation problems.First, we consider the two-dimensional problem of the normal impact of a hemispherical-nosed, hard steel rod against a block of 6061-T651 aluminum. Experimental data, along with analytical estimates of penetration depth, were obtained for this problem for a number of impact velocities by Forrestal, Brar, and Luk (1991). Details of the experiment may be obtained from this reference. These authors performed careful characterization of the hardening behavior of the target material from large strain compressive stress-strain curves for the particular material used in the experiment.

The CTH calculation used square cells of width 0.4 mm in the vicinity of the path of the penetrator. The rod itself was 7.11 mm in diameter and 71.12 mm in length, so there were about 9 cells across the radius of the rod. The density of the rod, which was 8000 kg/m^3 in reality, was modified by the correction factor shown in Equation1 as discussed in the preceding section. The Young's modulus of the rod was 205 GPa, and the Poisson's ratio was 0.3. The target material had a density of 2700 kg/m^3, a Young's modulus of 80 GPa, and a Poisson's ratio of 0.33. The hardening rule for the target material was represented by the relation

$$Y = A\,(1 + B\varepsilon^p)^n \qquad \text{(EQ 2)}$$

where Y is flow stress, ε^p is equivalent plastic strain, and A, B, and n are constants, A=276 MPa, B=249.6, and n=0.051.

Figure 3.1a shows the initial configuration. Figure 3.1b shows the final configuration for an impact velocity of 959 m/s. A friction coefficient of 0.06 was used. This value was found by trial and error to result in the best agreement between CTH and the experimental data over a wide range of impact velocities. Figure 3.2 shows the predicted penetration depth as a function of impact velocity, along with the experimentally measured values. All the computations used a friction coefficient of 0.06, except for one that had no friction. Note the large effect on penetration depth obtained by omitting friction shown in Figure 3.2.

The next example problem we consider is the grazing incidence of a linearly elastic sphere of mass 3.11 g and diameter 13 mm against a slab of aluminum. This problem was modeled in three dimensions with CTH. The projectile and target materials both had a density of 2700 kg/m^3, a Young's modulus of 80 GPa, and a Poisson's ratio of 0.3. The target material had a constant flow stress of 0.5 GPa. The impact velocity was 2.0 km/s, and the friction coefficient was 0.1. The cells were cubic with edge length 0.6 mm, so there were approximately 11 cells across the radius of the projectile.

Figures 3.3a,b show the initial configuration and the configuration after 25 μs. Note the bounce of the projectile off the surface, leaving a long gouge behind it. The dark shaded bar visible within the cross-section of the projectile is there merely to indicate rotation. The sphere evidently starts to rotate following impact. This makes sense physically, because friction would impart a non-zero angular momentum to the body. Unfortunately, the rotation is also partially due to numerical errors, since, as discussed in the previous section, the boundary layer algorithm tends to enlarge the projectile wherever it comes into contact with the target.

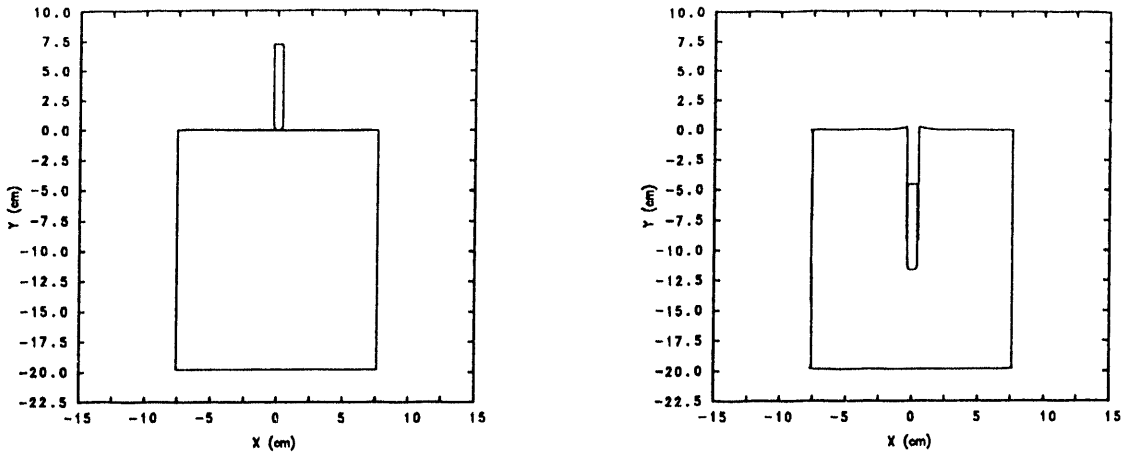

Figure 3.1. (a) Initial configuration for the CTH simulation of the penetration of an aluminum block by a steel rod. (b) Final configuration.

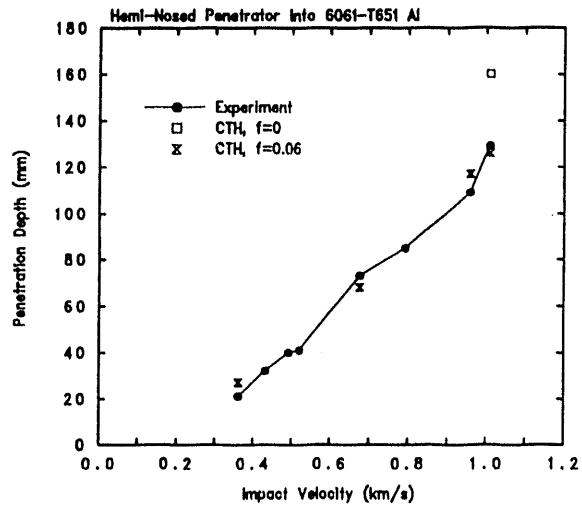

Figure 3.2. Predicted penetration depth as a function of impact velocity, along with experimental measurements (Forrestal, Brar, and Luk, 1991), for the penetration of aluminum by steel rods.

The next example problem is similar to the previous one, but the angle of incidence is 45 degrees, and the mass of the projectile is 9.20 g. (The density of the projectile was increased to 8000 kg/m^3, while the other material properties remained the same as in the previous example.) As shown in Figures 3.4a,b, in this case the sphere penetrates the target rather than ricocheting. The latter figure shows the configuration after 30 μs (the projectile is still moving).

The next problem is the perforation of an aluminum plate by a linear elastic, hemispherical-nosed rod. The target is 20 mm thick and is assumed to be elastic-perfectly plastic with a yield stress of 0.5 GPa. The rod is 8 mm in diameter and 40 mm long. The impact velocity of 1.5 km/s is normal to the plate, but there is a 10 degree yaw angle. The rod has a density of 7900 kg/m^3, a Young's modulus of 200 GPa, and a Poisson's ratio of 0.3. The target material has a density of 2700 kg/m^3, a Young's modulus

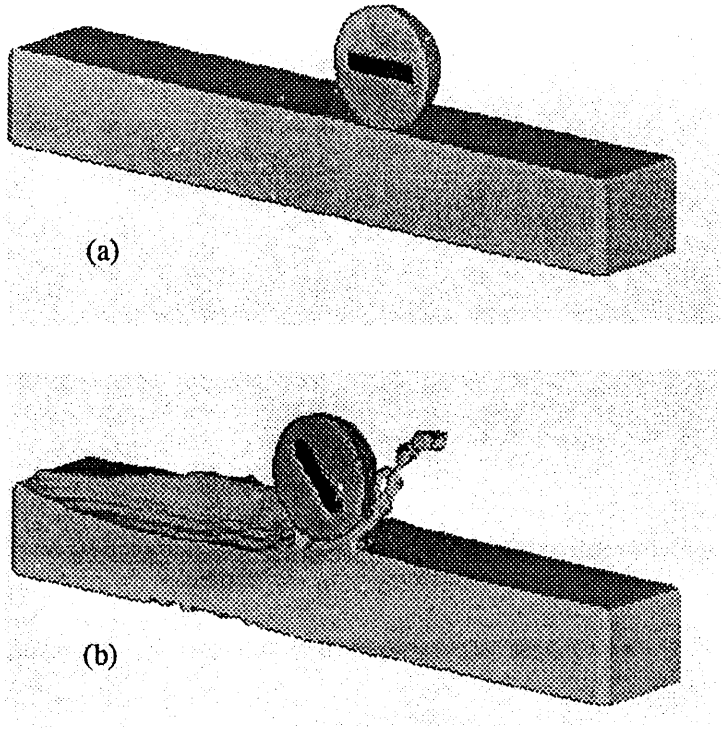

Figure 3.3. Linear elastic sphere impacting an aluminum slab at a 10 degree angle of incidence from the horizontal. (a) Initial configuration. (b) After 25 μs.

of 80 GPa, a Poisson's ratio of 0.3, and a constant flow stress of 0.5 GPa. Figures 3.5a,b show the initial configuration and the computed result after 31.5 μs. Note the large elastic strains present in the rod, reflecting the enormous shear stresses (on the order of 5 GPa).

Finally, we consider the same problem, but we assume in this case that the rod is elastic-perfectly plastic, with a yield stress of 2.5 GPa, which is characteristic of very high strength steel. The other material properties of both materials remain the same as in the previous example. Figure 3.5c shows the resulting configuration predicted after 35 μs. Note the extensive erosion of the rod.

4.0 Conclusions

This paper has summarized the progress being made in the specialization and application of CTH to problems involving penetration and perforation of materials by solids at relatively low (less than about 1.5 km/s) impact velocities. The suitability of the code for these applications has been enhanced

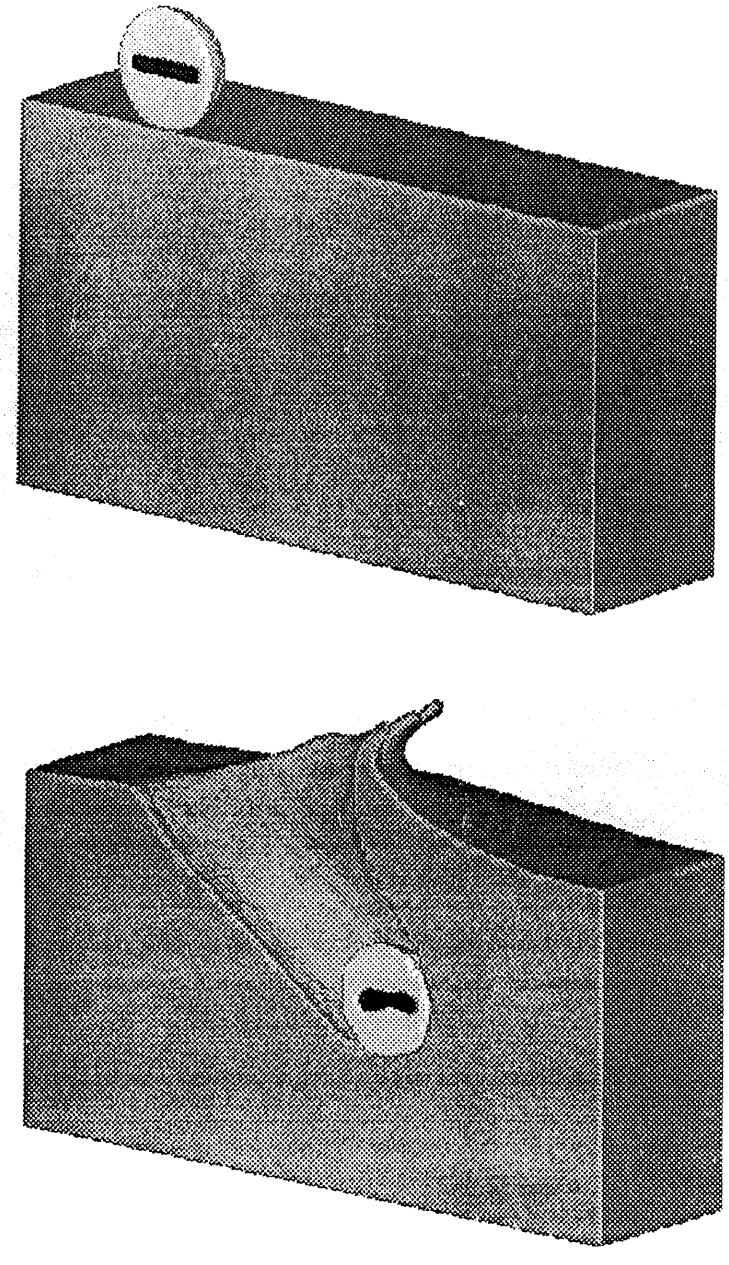

Figure 3.4. Impact of a linear elastic sphere at a 45 degree angle of incidence. (a) Initial configuration. (b) After 30μs.

by the introduction of a new algorithm for the modeling of sliding interfaces between solids, known as the boundary layer algorithm. This algorithm has the advantage over Lagrangian slidelines of not requiring elaborate searching procedures and complex geometrical descriptions of the configuration along the interface. It has the disadvantage of introducing, in effect, small changes in shape of the penetrator. However, these changes in shape can be corrected for when necessary.

In general, an Eulerian code like CTH requires a finer mesh than a Lagrangian code to achieve the same level of accuracy in a penetration or perforation problem involving solids. However, the problems of mesh distortion and the resulting need to rezone in order to keep the time increment size viable are eliminated with the Eulerian approach.

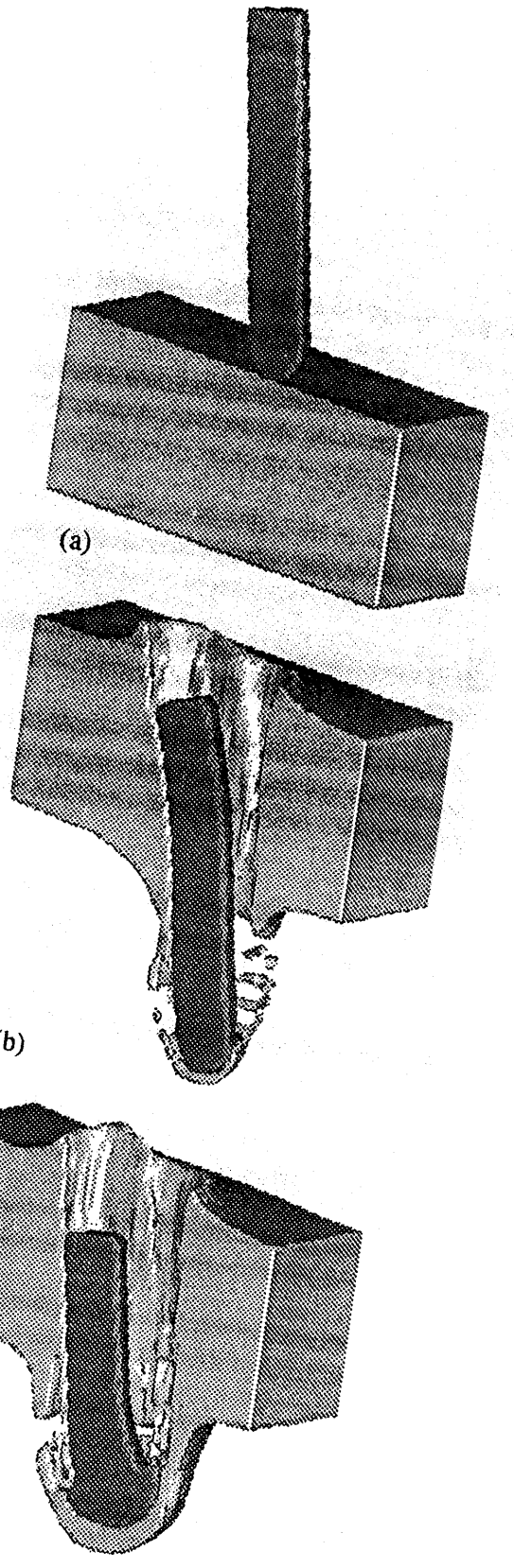

Figure 3.5. Normal incidence of a rod against an aluminum plate, 10 degree yaw angle. (a) Initial configuration. (b) Linear elastic rod. (c) Elastic-plastic rod.

ACKNOWLEDGMENT

This work performed at Sandia National Laboratories supported by the U.S. DOE under contract #DE-AC04-76DP00789.

5.0 References

M. J. Forrestal, N. S. Brar, and V. K. Luk (1991), "Penetration of Strain-Hardening Targets With Rigid Spherical-Nose Rods," *J. Appl. Mech.* **56**, pp. 7-10.

W. Herrmann and L. D. Bertholf (1983), "Explicit Lagrangian Finite-Difference Methods," in *Computational Methods for Transient Analysis*, T. Belytschko and T. J. R. Hughes, eds., Amsterdam, Elsevier Science Publishers, pp. 361-416.

G. R. Johnson and W. H. Cook (1983), "A Constitutive Model and Data for Metals Subjected to Large Strains, High Strain Rates and High Temperatures," in *Seventh International Symposium on Ballistics, The Hague, Netherlands*, pp. 541-547

G. R. Johnson and W. H. Cook (1985), "Fracture Characteristics of Three Metals Subjected to Various Strains, Strain Rates, Temperatures, and Pressures," *Engrg. Frac. Mech.* **21**, pp. 31-48.

G. R. Johnson, T. J. Holmquist, J. Lankford, C. E. Anderson, and J. Walker (1990), "A Computational Constitutive Model and Test Data for Ceramics Subjected to Large Strains, High Strain Rates, and High Pressures, Technical Report, Contract DE-AC04-87AL-42550, Honeywell, Inc., Brooklyn Park, MN.

G. R. Johnson and R. A. Stryk (1990), "User Instructions for the 1990 Version of the Combined (1D, 2D, 3D) EPIC Code," Technical Report, Contract DE-AC04-87AL-42550, Honeywell, Inc., Brooklyn Park, MN.

G. I. Kerley (1991), "CTH Reference Manual: The Equation of State Package," Technical Report SAND91-0344, Sandia National Laboratories, Albuquerque, NM.

J. M. McGlaun, S. L. Thompson, and M. G. Elrick (1990), "CTH: A Three-Dimensional Shock Wave Physics Code," *Int. J. Impact Engrg.* **10**, pp. 351-360.

S. A. Silling (1992a), "Eulerian Simulation of the Perforation of Aluminum Plates by Nondeforming Projectiles," Technical Report SAND92-0493, Sandia National Laboratories, Albuquerque, NM.

S. A. Silling (1992b), "An Algorithm for Eulerian Simulation of Penetration," in: *New Methods in Transient Analysis*, ASME, PVP-Vol. 246, AMD-Vol. 143, pp. 123-128.

D. J. Steinberg, S. G. Cochran, and M. W. Guinan (1980), "A Constitutive Model for Metals Applicable at High-Strain Rate," *J. Appl. Phys.* **51**, pp. 1498-1504.

D. J. Steinberg and C. M. Lund (1989), "A Constitutive Model for Strain Rates from 10^{-4} to 10^{6} s^{-1}," *J. Appl. Phys.* **65**, pp. 1528-1532.

B. Van Leer (1977), "Towards the Ultimate Conservative Difference Scheme IV. A New Approach to Numerical Convection," *J. Comp. Phys.* **23**, pp. 276-299

M. L. Wilkins (1969), "Calculation of Elastic-Plastic Flow," Technical Report UCRL-7322 (revised), Lawrence Radiation Laboratory, Livermore, CA.

F. J. Zerilli and R. W. Armstrong (1987), "Dislocation-Mechanics-Based Constitutive Relations for Material Dynamics Calculations," *J. Appl. Phys.* **61,** pp. 1816-1825.

DATE
FILMED
1/10/94
END